Journal of Alloys and Compounds 509 (2011) 2576–2581

Contents lists available at ScienceDirect

Journal of Alloys and Compounds

journal homepage: www.elsevier.com/locate/jallcom

Fabrication and evaluation of atmospheric plasma spraying WC–Co–Cu–MoS_2 composite coatings

Jianhui Yuan, Yingchun Zhu*, Xuebing Zheng, Heng Ji, Tao Yang

Key Laboratory of Inorganic Coating Materials, Shanghai Institute of Ceramics (SIC), Chinese Academy of Sciences (CAS), Dingxi 1295, Changning, Shanghai, 200050, China

ARTICLE INFO

Article history:
Received 10 March 2010
Received in revised form 28 October 2010
Accepted 16 November 2010
Available online 23 November 2010

Keywords:
Tribological property
WC–Co coating
Atmospheric plasma spraying
MoS2
Solid lubricant

ABSTRACT

Protective WC–Co-based coatings containing solid lubricant Cu and MoS_2 used in wear applications were investigated in this study. These coatings were deposited on mild steel substrates by atmospheric plasma spraying (APS). The feedstock powders were prepared by mechanically mixing the solid lubricant powders and WC–Co powder, followed by sintering and crushing the mixtures to avoid different particle flighting trajectories at plasma. The tribological properties of the coatings against stainless steel balls were examined by ball-on-disk (BOD) tribometer under normal atmospheric condition. The microstructure of the coatings was studied by optical microscope, scanning electron microscope and X-ray diffraction. It was found that the MoS_2 composition in the feed powder was kept in WC–Co–Cu–MoS_2 coatings, and the decomposition and decarburization of WC in APS process were improved, which were attributed to the protection of Cu around them. The friction and wear behaviors of all the WC–Co–Cu–MoS_2 coatings were superior to that of WC–Co coating. Such behavior was associated to different wear mechanisms operating for WC–Co coating and the WC–Co–Cu–MoS_2 coatings.

1. Introduction

Aircraft, textile, automobile and mining are some of the areas where coatings offering a lower friction and a longer lifetime are required [1]. To satisfy the industrial demands for high performance coatings, improved and application adapted coatings are developed. WC–Co is one of the most common materials in a variety of applications where high levels of wear resistance is required and has been in use since the 1930s [2]. However, one noticeable problem is that its high hardness and strength increase the wear rate of the counter face and lead to high friction coefficient sometimes [3]. To be accepted as a more general tool material, however, WC–Co requires significant modification to bring about improvement on frictional characteristic [4].

Many efforts, such as developing new spray methods [5], minimizing the size of the spray powders [6], have been made to improve the friction properties of WC–Co coating. However, Usmani et al. [7], and Stewart et al. [8] reported disappointing sliding wear and abrasive wear resistances of nanostructured WC–Co coatings for the increased decarburization. One promising way to improve wear resistance of thermal sprayed coatings is self-lubrication by doping lubricant in them, which is cheaper and easier than the optimization for nanostructured coatings [9]. Self-lubricating composites were introduced by Alexeyev and Jahanmir [10]. MoS_2 is a well-known solid lubricant used widely as tribological coatings, especially for applications in vacuum or dry environment [11]. Combining the wear resistance of WC with the lubricating properties of MoS_2 has an extremely beneficial effect on improving the tribological performance of the resulting coating in the future.

Thermal spraying is an economical method of depositing coatings which have extensive applications in many fields such as wear and corrosion resistance [12]. It is a common practice to deposit WC–Co surface coatings by thermal spraying, typically atmospheric plasma spraying (APS) [13]. In order to combine the satisfactory lubricating property of MoS_2 with the high wear resistance of WC–Co, coatings mixing both components are produced by APS. However, the biggest challenge of this method is to retain the preexisting lubricant in feed powder from chemical reaction at the high temperature in APS. In the present study, MoS_2 composition will be kept due to the protection of Cu added to the feed powder. Furthermore, the Cu added to the feed powder will inhibit the decomposition of WC and offer lubricating function. However, few reports on doping lubricant in the feed powder to improve the wear properties of thermal sprayed coatings have been published. In our work, WC–Co powder mixed with various weight percentages of Cu and MoS_2 powders are deposited by APS under a proper spraying condition. The sliding wear property of the resulting composite coatings is evaluated by a ball-on-disc tester.

* Corresponding author. Tel.: +86 21 52412632; fax: +86 21 52412632.
E-mail address: yzhu@mail.sic.ac.cn (Y. Zhu).

0925-8388/$ – see front matter © 2010 Elsevier B.V. All rights reserved.
doi:10.1016/j.jallcom.2010.11.093

Table 1
Nomenclature of the samples used in this study.

Samples nomenclature	Description
WC–Co coasting	Deposited using WC–Co powder
90W6C4S coating	Deposited using 90 wt.%WC–Co–6 wt.%Cu–4 wt.%MoS_2 composite power
80W12C8S coating	Deposited using 80 wt.%WC–Co–12 wt.%Cu–8 wt.%MoS_2 composite power
70W18C12S coating	Deposited using 70 wt.%WC–Co–18 wt.%Cu–12 wt.%MoS_2 composite power

2. Experimental procedures

2.1. Thermal spray feedstock materials

The WC–Co alloy powder selected to prepare the coatings had a composition of WC–12%Co (Chengdu Daguang Thermal Spraying Material Co. Ltd.). The mean particle size was in the range of 15~45 μm. MoS_2 (LUBTOP) and Cu (Sinopharm Chemical Reagent Co., Ltd.) powders with an average size of 3~4 μm and 15~50 μm, respectively, were employed as doping powder for the resulting coating. First, the original powders were wet milling for 24 h in a ball mill, then the mixed powders were sintered for 2 h at 1100 °C in a vacuum electrical furnace. The sintered composite bulks were then crushed and separated by a 200 mesh screen. The powder with a size less than 200 mesh was used as feedstock material for thermal spray. In order to investigate the effect of content of lubricant in WC–Co–Cu–MoS_2 coatings on sliding wear property, WC–Co powder mixed with various weight percentages of Cu and MoS_2 powders were deposited with a proper spraying condition. In the present study, three different kinds of WC–Co–Cu–MoS_2 coating samples were investigated. And the WC–Co coating was also examined for comparison. The obtained coating samples nomenclature and their description are presented in Table 1.

2.2. Thermal spraying process

The coatings were obtained by atmospheric plasma spraying (APS) using a spraying system consisting of a F4-MB plasma spray gun (Sulzer Metco) mounted on an S3 robot (ABB). Prior to depositing the coatings, the surface of the mild steel substrates were grit-blasted with silicon carbide grits in order to produce a rough surface for good bonding. Coating samples, with thicknesses of about 300 μm, were deposited onto the mild steel substrates by APS. Table 2 showed the optimized spraying conditions adopted in the present work.

2.3. Sliding wear tests

The friction and wear tests without lubrication were conducted on a ball-on-disk tribometer. Prior to the wear tests, the disc samples with dimension of Ø 60 mm × 5 mm were covered with WC–Co coating or WC–Co–Cu–MoS_2 composite coating. 302 stainless steel balls 4 mm in diameter with a bulk hardness of RC39 were used as the counter face balls. The coating samples were prepared by grinding and final polishing with a diamond paste achieving a surface roughness of Ra = 0.5 μm, then cleaned with acetone in an ultrasonic cleaner and dried before testing. The wear tests were carried out under a dry sliding condition, at a sliding velocity of 0.5 m/s for a sliding distance of 600 m. The normal load was 10 N. The environmental conditions of relative humidity and temperature 63% and 25 °C, respectively, were held constant during the test.

The friction coefficient μ was got directly by the tester. A HOMMEL TESTERT8000 Surface Profilometer was used to determine the cross-sectional areas of wear tracks. Based on the diameter and the cross-sectional area of wear track at several locations, the coating volume removed (ΔV) during the testing was obtained, and the specific wear rate W was determined according to Eq. (1):

$$W = \frac{\Delta V}{PL} \quad (1)$$

where L was the sliding distance and P was the normal load applied. Both the friction coefficients and wear rates were obtained by averaging over three specimens.

Table 2
The atmospheric plasma spraying parameters.

Current (A)	Voltage (V)	Ar (SPLM)	H_2 (SPLM)	Powder feed rate (r/min)	Spraying distance (mm)
400	55	50	3	14	100

2.4. Characterization of coatings and worn surfaces

X-Ray spectra of the powder as well as the sprayed coatings were acquired by an X-ray diffraction (D/Max 2200 VPC) using Cu Kα radiation to provide a qualitative identification of the phase present. The peaks were scanned with a 2θ step of 0.02°/s from 30° to 80°. Then the peaks of each phase were indexed using available standard XRD data. Microscopic observation of the coatings before and after wear was performed using an optical microscope (Olympus B071) and a scanning electron microscopy (SEM; JEOL JXA-8100) equipped with energy-dispersive spectroscopy (EDS) and wavelength dispersive spectroscopy (WDS).

3. Results and discussion

3.1. Microstructure and composition of the coatings

Fig. 1 shows the XRD patterns of WC–Co coating and WC–Co–Cu–MoS_2 coatings. WC peak is of great intensity in all coatings. In WC–Co coating, the W_2C-major peak is of much higher intensity than the WC major peak, and peaks from metallic W and Co_6W_6C are also present (Fig. 1(a) [14]. It is concluded that the decarburization of WC–Co powder occurred in atmospheric plasma spraying. The presence of decarburized WC and complex carbides in plasma sprayed coatings, as noted in the present work, is consistent with the observational results of Subramanyam et al. [15], Lenling et al. [16], and Provot et al. [17]. However, the XRD pattern shows a reduced intensity of W_2C peaks in Fig. 1(b)–(d), indicating that the degree of WC decomposition is lower in WC–Co–Cu–MoS_2 coatings [18]. Moreover, the W_2C peaks remarkably decrease in intensity with increasing Cu and MoS_2 content. It suggests that the Cu outer layer can minimize the degree of WC decomposition. The peaks for MoS_2 phase are detected for all composite coatings produced with the powders containing MoS_2 composite, while no peak for oxide of MoS_2 or other phase is found. The maintenance of MoS_2 and WC phases in the resulting coating can be attributed to the protection of Cu.

The position and distribution of elements in the 70W18C12S coating detected by SEM-WDS are shown in Fig. 2. Fig. 2(a) is the topographic feature of the composite coating. Fig. 2(b)–(d) show the elements distributing cases on the micro-area in Fig. 2(a), respectively. It can be observed that W covers most parts of the micro-area (Fig. 2(c)). WDS in conjunction with SEM indicates that WC parti-

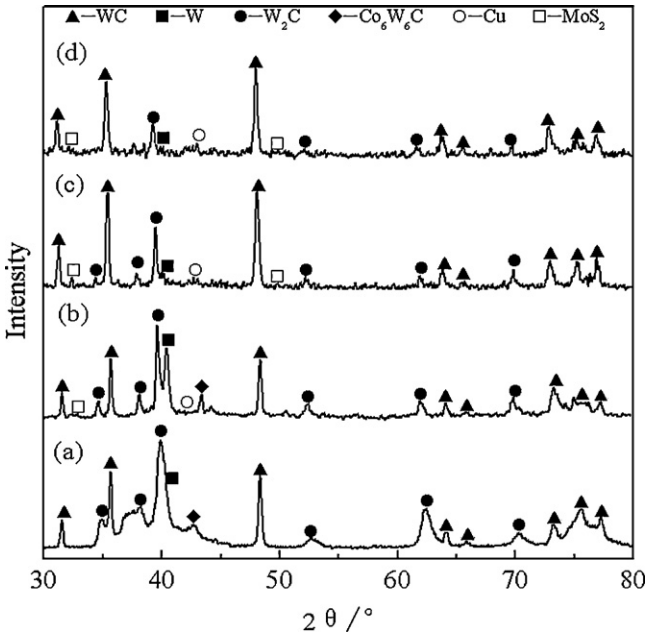

Fig. 1. XRD patterns for the (a) WC–Co coating; (b) 90W6C4S coating; (c) 80W12C8S coating and (d) 70W18C12S coating.

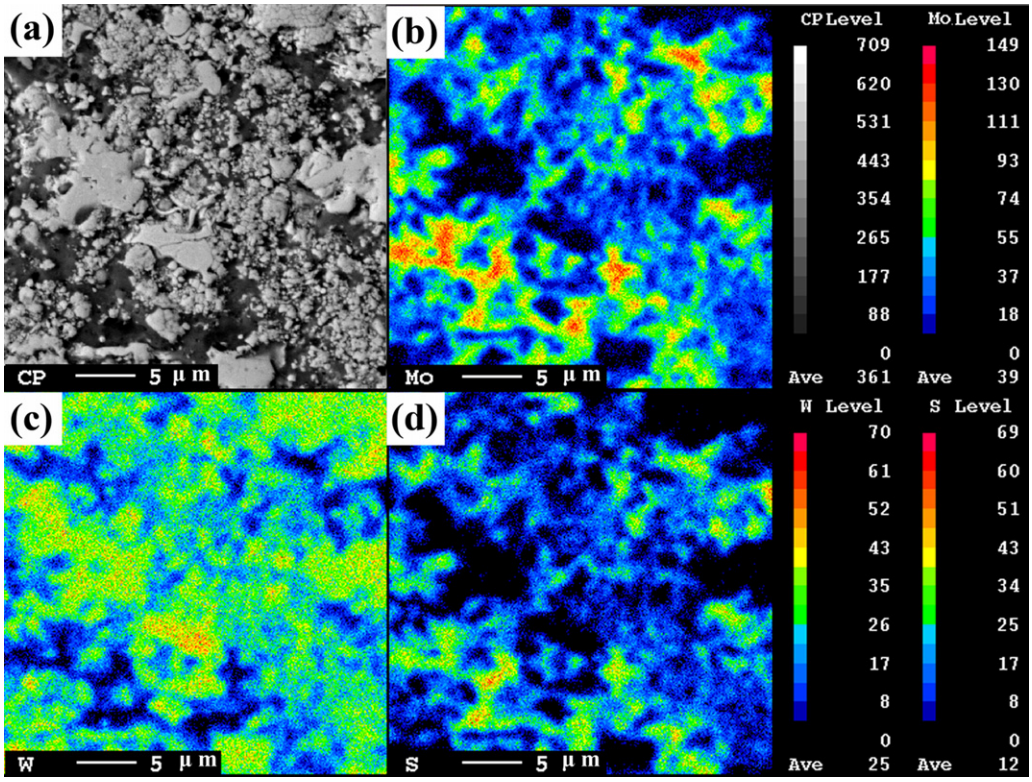

Fig. 2. SEM and WDS analysis of the 70W18C12S coating (a) SEM micrograph and distribution of (b) Mo, (c) W and (d) S.

cles formed a skeleton structure of the micro-area. The lubricating phase is embedded in the WC skeleton structure (Fig. 2(b) and (d)). Moreover, it is interesting to find that the two elements, Mo and S, have almost the same position in the coatings. Combining the SEM, XRD, and WDS results mentioned above, it can be inferred that the premise of this coating system, a solid lubricant phase (MoS_2) distributed in the WC–Co coating has been fulfilled.

Fig. 3 shows the backscattered electron imaging (BEI)-SEM micrographs of polished surface of WC–Co and WC–Co–Cu–MoS_2 coatings. All the coatings are composed of high levels of particulate

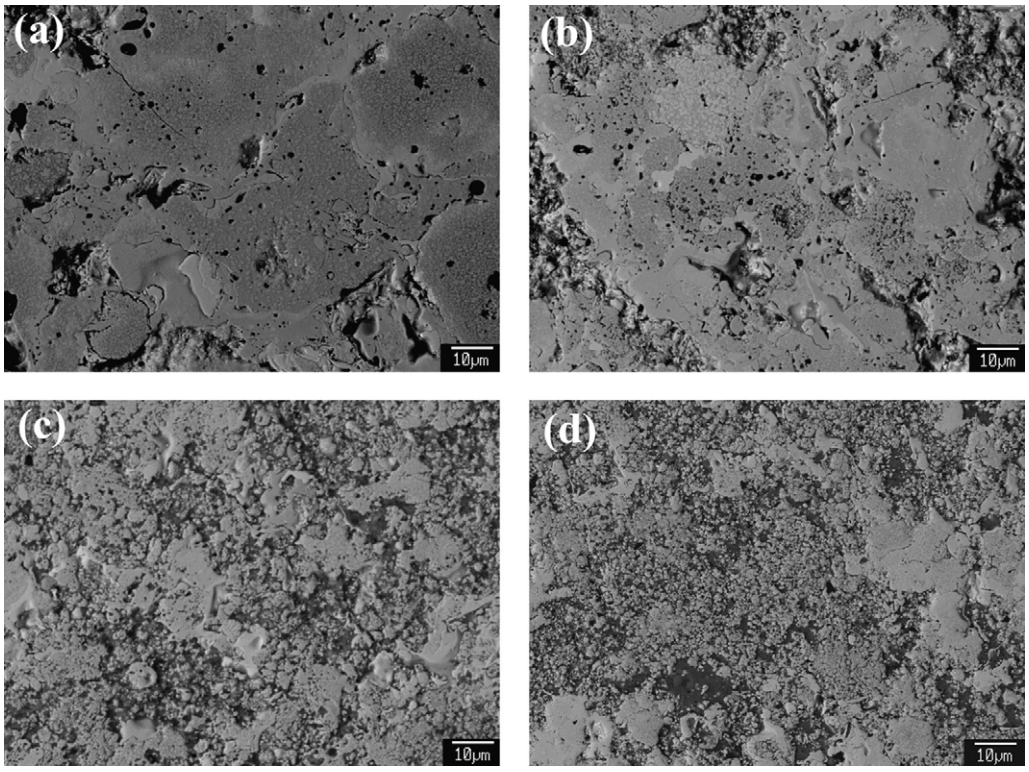

Fig. 3. SEM micrographs of polished surface of (a) WC–Co coating; (b) 90W6C4S coating; (c) 80W12C8S coating and (d) 70W18C12S coating.

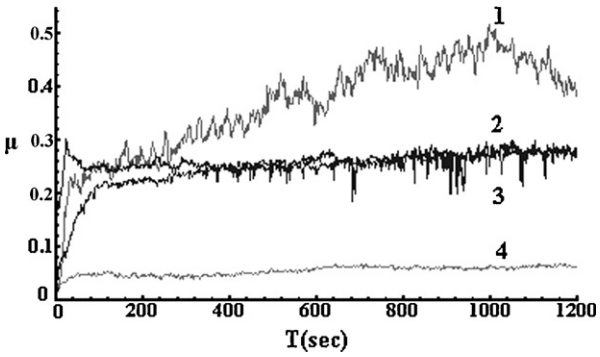

Fig. 4. Friction coefficients depending on sliding time of curve 1: WC–Co coating; curve 2: 90W6C4S coating; curve 3: 80W12C8S coating and curve 4: 70W18C12S coating against stainless steel ball.

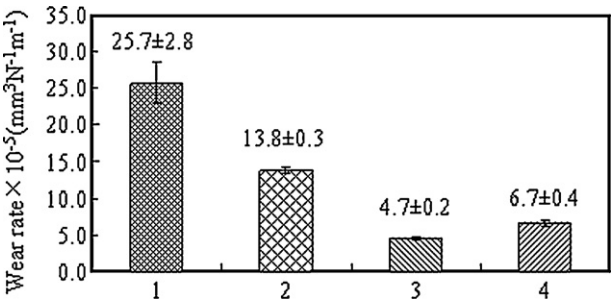

Fig. 5. Wear rates of column 1: WC–Co coating; column 2: 90W6C4S coating; column 3: 80W12C8S coating and column 4: 70W18C12S coating against stainless steel balls.

ceramic phase bound together with a metallic binder. The WC–Co coating clearly shows a platelet structure built up of many individual splats containing retained WC and large amounts of non-WC phases (Fig. 3(a)). A number of micro-pores and micro-cracks are also observed. Under BEI, the dark and bright regions correspond to regions of lower and higher mean atomic numbers, respectively. So these bright and dark binder layers in WC–Co coating are known as W-rich and Co-rich regions, respectively [19]. These inhomogeneous compositions of the binder result from the dissolution of WC during spraying process and rapid cooling of the powders when they reach the substrate [20].

The SEM micrograph of 90W6C4S coating (Fig. 3(b)) is similar to that of WC–Co coating (Fig. 3(a)), which indicates that the addition of 4 wt.% MoS_2 and 6 wt.% Cu cannot change the microstructure of WC–Co coating evidently. But as the quantity of MoS_2 and Cu increase, the microstructure of composite coatings becomes much different from that of WC–Co coating. Both the 80W12C8S coating and 70W18C12S coating exhibit very dense structure with few small pore, as shown in Fig. 3(c) and (d). It also shows that the higher MoS_2 and Cu content is in the feed powder, the more gray layers appear in the resulting WC–Co–Cu–MoS_2 coatings. It can be concluded that the addition of MoS_2 and Cu into the plasma deposited WC–Co coating reduces the open porosity and makes the composite coatings more dense and compact.

3.2. Sliding wear behavior

The variation of the friction coefficients as functions of sliding time for WC–Co coating and WC–Co–Cu–MoS_2 coatings against stainless steel balls is shown in Fig. 4. It can be seen that the friction coefficients behave in a similar manner (curves 1, 2 and 3 in Fig. 4), whereby the friction coefficients rise rapidly from a low value during the running-in period (about 120 s) and then reach the steady-state value, except in the 70W18C12S coating (curve 4 in Fig. 4) where the friction coefficient reaches the steady-state value at quite an early stage (about 50 s). Comparing the steady-state friction coefficient values, it is clear that all the composite coatings still have much lower steady-state friction coefficients than that of WC–Co coating. And the steady-state friction coefficients decrease with the increase of Cu and MoS_2 contents. The WC–Co coating without solid lubricants exhibits the highest steady-state friction coefficient (about 0.38), while the composite with 18 wt.% Cu and 12 wt.% MoS_2 solid lubricants shows the lowest steady-state friction coefficient (about 0.06, an order of magnitude less) under the same test conditions. The decrease of the friction coefficient is attributed to the addition of Cu and MoS_2 in the coatings. Our previous work showed that Cu in WC–Co coating can decrease the friction coefficient to 0.18 [21]. It is noted that the friction coefficient is greatly decreased to 0.06 when MoS_2 was added to the coating, as shown in Fig. 4. Apparently, MoS_2 plays a very important role on the self-lubricating property of as-prepared composite coatings.

The wear rates of WC–Co coating and WC–Co–Cu–MoS_2 coatings sliding under the same condition are shown in Fig. 5. The error bars in the wear data indicate the scatter in the data (standard deviation) for at least five test results. It can be seen that the wear rates of the composite coatings are significantly lower than that of the WC–Co coating. The wear rate of WC–Co is high ($(25.7 \pm 2.8) \times 10^{-5}$ mm^3 N^{-1} m^{-1}) and it decreases with the increase of the Cu and MoS_2 contents. However, the wear rate of 70W18C12S coating is a little higher than that of 80W12C8S coating. Comparing to WC–Co coating, an improvement in wear-resistance of about 2 times is observed for 90W8C4S coating. The 80W12C8S and 70W18C12S coatings show an improvement in wear resistance of 5.4 and 3.8 times, respectively.

3.3. Worn surfaces analysis

After the sliding wear tests, the SEM micrographs of the worn surface of the WC–Co coating and WC–Co–Cu–MoS_2 coatings are shown in Fig. 6. The worn track on the WC–Co coating exhibits much more significant pitting and severe cracking (Fig. 6(a)), which shows large amounts of material loss from the worn track. The worn surface of the 90W6C4S coating is roughened and uneven with much pits (Fig. 6(b)), which suggests that the splat delamination is quite intense. In contrast, Fig. 6(c) shows comparatively smooth worn surfaces with a little of pits. And cracks or pits are not observed in Fig. 6(d). The worn surfaces of 80W12CS coating and 70W18C12S coating do not exhibit large scale fracture or damage as have been seen in WC–Co coating. Continuous triboreaction layers formed on the two surfaces are observed. The triboreaction layer of 70W18C12S coating is denser than that of 80W12C8S coating.

In order to investigate the wear mechanism, the worn surface of 70W18C12S coating is further studied by the BEI and associated EDS. It is clear that the triboreaction layer smears on the worn surface of 70W18C12S coating, as shown in Fig. 7(a). The triboreaction layer of 70W18C12S coating mainly contains W, Cu, Mo, S, Fe, Cr and O (Fig. 7(b)), which implies that the triboreaction layer is consisted of small WC particles, oxidized stainless steel constituents, Cu and MoS_2 lubricants. The presence of small quantity of O may be due to the oxidization of surface materials at high flash temperature in the sliding wear tests. The Fe and Cr contents in the worn surfaces reflect the degree of counter face balls scraped by the WC particles that protrude out of the composite contacting surfaces. In summary, the triboreaction layer is formed by compaction and mixing of material removed from the stainless steel ball and the composite coating.

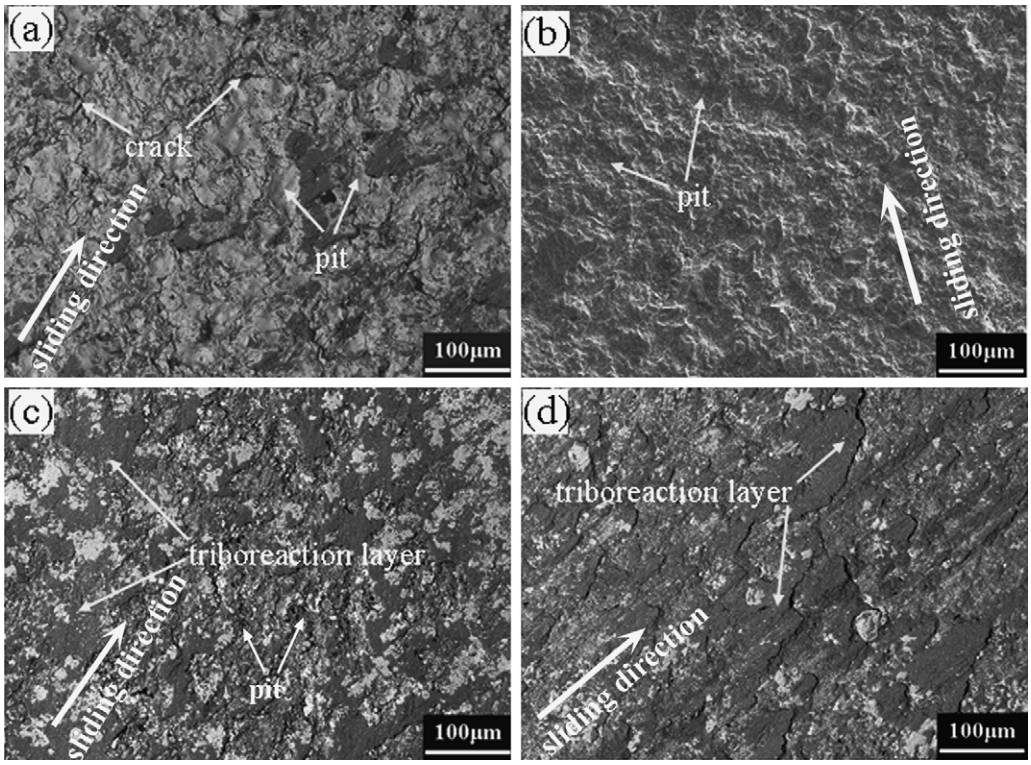

Fig. 6. SEM morphologies of worn surface of the (a) WC–Co coating; (b) 90W6C4S coating; (c) 80W12C8S coating and (d) 70W18C12S coating against the stainless steel ball.

3.4. Discussion

The primary features of the atmospheric plasma sprayed WC–Co coating are a large number of scattered cavities and defects (Fig. 3(a)). Besides, the decarburized WC and complex carbides present in plasma sprayed coatings are brittle in nature and detrimental to wear resistance [22]. In the sliding wear tests, the WC–Co coating is subjected to alternately tensile and compression stress and the cracks will initiate in the subsurface, where they suffer the maximum shear stress. When these subsurface cracks propagate through the bind phase or along the splat boundary where the brittle decarburized phases exist, material removal occurs [23,24]. The wear behavior is controlled by the brittleness of the coatings. Therefore, it is known that the wear rate of WC–Co coating is governed by fatigue wear mechanism dominated by fracture involving crack nucleation and propagation.

The addition of Cu and MoS_2 to the plasma deposited WC–Co coating increases the bind phases remarkably, leading to the reduction of porosity and elimination of the defects. Furthermore, the Cu layer can avoid the direct exposure of WC into the oxidizing flame environment effectively, and the degree of WC decomposition is much lower in the WC–Co–Cu–MoS_2 coatings. The addition of Cu also strengthens the binding of carbides to the matrix, thereby improves the crack propagation resistance as compared with WC–Co coatings. Therefore, fatigue wear can be avoided in the WC–Co–Cu–MoS_2 coatings [25].

MoS_2 has a highly anisotropic crystal layer structure, which consists of a layer of molybdenum atoms arranged in a hexagonal array with each molybdenum atom surrounded at equal distance by six sulfur atoms placed at the corners of a triangular prism. Within the MoS_2 'sandwiches' there is strong covalent bonding, but between the sandwiches only weak Van der Waals' forces exist. This weak

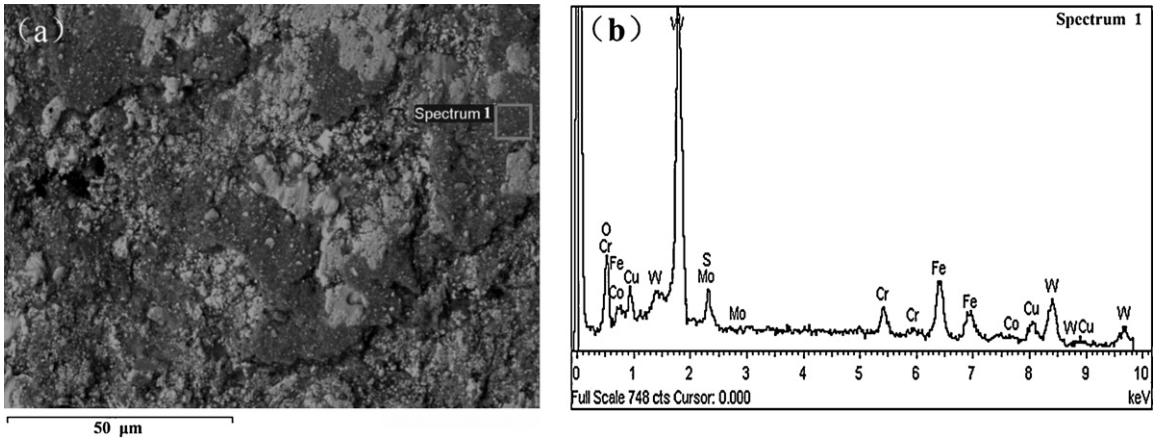

Fig. 7. The BEI and associated EDS of the worn surface: (a) 70W18C12S coating and (b) EDS of the triboreaction layer in (a).

bonding between layers of MoS_2 results in low shear strength, and hence low friction in the sliding direction. So, the friction reducing effect of MoS_2 in the WC–Co–Cu–MoS_2 coatings lasts for the whole sliding process, which results in the improved wear resistance of the composite coatings.

Since the frictional heat leads to an instantaneous temperature rise at the contacting surface, the material of counter body transfers to the sliding surface easily. A tribochemistry reaction will occur between the counter body material and the coating material. The product of the reaction is deposited initially in the porosity. However, when all the pores are filled with the product, it adheres to some of the coating and a triboreaction layer is formed, as shown in Fig. 7. According to the analysis above, it can be concluded that a triboreaction layer contains fragments of the WC, the smeared counter body and the lubricants. Therefore, as the contents of Cu and MoS_2 increase in the composite coatings, the triboreaction layer forms more easily and contains more lubricant. And the triboreaction layer acts as a lubricant and results low friction coefficient during friction process. Thus the friction coefficients for all composite coatings decrease (from 0.24 to 0.06) with the increase of lubricant content. When a successive and dense triboreaction layer is formed, the abrasion is reduced to some extent. However, the further increase in the contents of Cu and MoS_2 will lead to excess triboreaction product which will act as an abrasive because of its deforming and hardening. This kind of abrasive produces higher wear of the coating according to a three-body abrasive wear mechanism [26]. Therefore, the wear rate of 70W18C12S coating is a little higher than that of 80W12C8S coating in this research.

4. Conclusions

A series of WC–Co–Cu–MoS_2 coatings were deposited using homemade feedstock powders composed of WC–Co, Cu and MoS_2 by atmospheric plasma spraying. The results obtained by SEM, XRD, EDS and WDS indicated that the MoS_2 composition was kept and distributed homogeneously in the WC–Co–Cu–MoS_2 coatings. The lower degree of WC decomposition and decarburization in the WC–Co–Cu–MoS_2 coatings were attributed to the protection of Cu. Because of the friction reducing effect of MoS_2, the WC–Co–Cu–MoS_2 coatings have a higher wear resistance than WC–Co coating. The material loss of the composite coatings was mainly governed by an abrasive wear mechanism, while the wear rate was governed by fatigue wear mechanism in WC–Co coating. As the increase of the content of lubricant in the composite coatings, a successive and dense triboreaction layer was formed and acted as a lubricant. However, the excess triboreaction product acted as an abrasive and led to higher wear during friction process. The results in this preliminary study promise that the envisioned deposition of WC–Co coating with self-lubricating property is feasible and the resulting coating can exhibit higher sliding wear resistance.

Acknowledgements

The research was partially financially supported from the National Natural Science Foundation of China (50772125), the Science and Technology Commission of Shanghai Municipality (08JC1420700), and the National High Technology Research and Development Program (863 Program) of China.

References

[1] T.N. Rhys-Jones, Surface and Coatings Technology 43–44 (1990) 402.
[2] P.H. Shipway, L. Howell, Wear 258 (2005) 303.
[3] Z.F. Zhang, L.C. Zhang, Y.W. Mai, Wear 176 (1994) 231.
[4] P. Chivavibul, M. Watanabe, S. Kuroda, M. Komatsu, Surface and Coatings Technology 202 (2008) 5127.
[5] H.-J. Kim, C.-H. Lee, S.-Y. Hwang, Materials Science and Engineering A 391 (2005) 243–248.
[6] Y.C. Zhu, C.X. Ding, K. Yukimura, T. DannyXiao, Perter R. Strutt, Ceramics International 27 (2001) 669–674.
[7] S. Usmani, S. Sampath, D.L. Houck, D. Lee, Tribology Transactions 40 (3) (1997) 470.
[8] D.A. Stewart, P.H. Shipway, D.G. McCartney, Wear 225–229 (1999) 789.
[9] H. Du, C. Sun, W.G. Hua, Y.S. Zhang, Z. Han, T.G. Wang, J. Gong, S.W. Lee, Tribology Letters 23 (3) (2006) 261–266.
[10] N. Alexeyev, S. Jahanmir, Wear 166 (1993) 41.
[11] O. Smorygo, S. Voronin, P. Bertrand, I. Smurov, Tribology Letters 17 (4) (2004) 723–726.
[12] P. Fauchais, G. Montavon, M. Vardelle, J. Cedelle, Surface and Coatings Technology 201 (2006) 1908–1921.
[13] A.K. Basak, S. Achanta, M. De Bonte, J.P. Celis, M. Vardavoulias, P. Matteazzi, Transactions of the Institute of Metal Finishing 85 (6) (2007) 310–315.
[14] W. Jun, L. Ke, S. Da, H. Xin, S. Baode, G. Qixin, N. Mitsuhiro, O. Hiroshi, Materials Science and Engineering A 371 (2004) 187–192.
[15] J. Subramanyam, M.P. Srivastava, R. Sivakumar, Materials Science and Engineering 84 (1986) 209.
[16] W.J. Lenling, M.F. Smith, J.A. Henpling, Proceeding National Thermal Spraying Conference, Long Beach, CA, USA, May 1990, ASM International, 1990, p. 227.
[17] X. Provot, H. Burlet, M. Vardavoulias, M. Jeandin, C. Richard, J. Lu, D. Manesse, Proceeding National Thermal Spraying Conference, Anaheim, CA, USA, June 1993, ASM International, 1993, p. 159.
[18] B.H. Kear, G. Skandan, R.K. Sadangi, Scripta Materialia 44 (2001) 1703–1707.
[19] D.A. Stewart, P.H. Shipway, D.G. McCartney, Acta Materialia 48 (2000) 1593.
[20] B.H. Kear, G. Skandan, R.K. Sadangi, Scripta Materialia 44 (2001) 1705.
[21] Y. Jianhui, Z. Yingchun, Z. Xuebing, R. Qichao, J. Heng, Applied Surface Science 255 (2009) 7959–7965.
[22] R. Nieminen, P. Vuoristo, K. Niemi, T. Mantyla, G. Barbezat, Wear 212 (1997) 69.
[23] D. Lingzhong, X. Binshi, D. Shiyun, Z. Weigang, Z. Jingmin, Y. Hua, W. Haijun, Surface and Coatings Technology 202 (2008) 3714.
[24] D. Hao, S. Chao, H. Weigang, W. Tiegang, G. Jun, J. Xin, W.L. Soo, Materials Science and Engineering A 445–446 (2007) 133.
[25] L. Prchlik, S. Sampath, J. Gutleber, G. Bancke, A.W. Ruff, Wear 249 (2001) 1103–1115.
[26] J.M. Guilemany, J.M. Miguel, S. Vizcaino, F. Climent, Surface and Coatings Technology 140 (2001) 141–146.